Journal of Solid State Chemistry 183 (2010) 2720–2725

Contents lists available at ScienceDirect

Journal of Solid State Chemistry

journal homepage: www.elsevier.com/locate/jssc

One pot synthesis of Ag nanoparticle modified ZnO microspheres in ethylene glycol medium and their enhanced photocatalytic performance

Chungui Tian, Wei Li, Kai Pan, Qi Zhang, Guohui Tian, Wei Zhou, Honggang Fu*

Key Laboratory of Functional Inorganic Material Chemistry, Ministry of Education of the People's Republic of China, Heilongjiang University, Harbin 150080, PR China

ARTICLE INFO

Article history:
Received 9 June 2010
Received in revised form
8 September 2010
Accepted 15 September 2010
Available online 19 September 2010

Keywords:
Photocatalysis
ZnO
Ag modification
Composites
One-pot synthesis

ABSTRACT

Ag nanoparticles (NPs) modified ZnO microspheres (Ag/ZnO microspheres) were prepared by a facile one pot strategy in ethylene glycol (EG) medium. The EG played two important roles in the synthesis: it could act as a reaction media for the formation of ZnO and reduce Ag^+ to Ag^0. A series of the characterizations indicated the successful combination of Ag NPs with ZnO microspheres. It was shown that Ag modification could greatly enhance the photocatalytic efficiency of ZnO microspheres by taking the photodegradation of Rhodamine B as a model reaction. With appropriate ratio of Ag and ZnO, Ag/ZnO microspheres showed the better photocatalytic performance than commercial Degussa P-25 TiO_2. Photoluminescence and surface photovoltage spectra demonstrated that Ag modification could effectively inhibit the recombination of the photoinduced electron and holes of ZnO. This is responsible for the higher photocatalytic activity of Ag/ZnO composites.

1. Introduction

Photocatalysis is one of the most dynamic areas in modern science as its potential in solving many current environmental and energy issues [1–3]. Semiconductor materials have received intensive interest in this area because their proper band gaps can effectively utilize light energy. Over the past few decades, most studies have been devoted into TiO_2 as their high photosensitivity and nontoxic nature [4,5]. Zinc oxides (ZnO), a direct wide band-gap (3.2 eV) semiconductor, have been considered as a suitable alternative to TiO_2 due to its similar band-gap energy with TiO_2 and lower cost [6,7]. When irradiation has energy greater than the band-gap energy of ZnO, the electrons in the valence band (VB) will be excited to the conduction band (CB), and thus form electron–hole pairs. The photo-induced electrons and holes are able to activate the surrounding chemical species and then promote the chemical reactions. It was shown that the photocatalytic performance of ZnO is affected by its crystallite size, specific surface area, morphologies and textures [8–17]. For example, Ghosh's group research showed that the photocatalytic activity of ZnO decreases as the particle size increases [13]. The dependence of the photocatalytic activity on the type and concentration of oxygen defects were studied by Zheng et al. [14]. Also, the face-dependent photocatalytic performance was explored by Jang et al.'s [15], Mclaren et al.'s [16] and Zheng's groups [17], respectively, and it was shown that (0001) and (000$\bar{1}$) facets of the hexagonal ZnO crystals have specific catalytic activity for photodegradation of organic contaminations. However, the rapid recombination of photo-induced hole–electron pairs is major obstacles for increasing photocatalytic efficiency of ZnO photocatalysts [18].

Nanoscience development provided great opportunity on the control over the chemical composition and surface modification of the materials [19–21]. Noble metal nanoparticles (NPs), such as Au, Ag, Pd and Pt, represent one of the most important areas in nanotechnology as their high stability and excellent properties [22]. The electronic structure of semiconductor is characterized by a VB filled with electrons and an empty CB, while those of metal NPs can be described as a sink for photoinduced charge [23]. Upon irradiation by an appropriate energy, the electrons promoted from VB to CB will be captured by the metal NPs contacting with the semiconductor particles, benefiting the separation of photo-generated carriers and improvement of the photoelectrochemical performances of the semiconductor particles [24]. The Pt–ZnO [25,26], Au–ZnO [27] and Ag–ZnO [28–33] composites were fabricated and their photocatalytic performance was also explored. The metal Ag is cheapest among all the noble metals. This should be favorable for its use in industrial scale. Several methods were developed to prepare the Ag–ZnO composites. For example, Ag NPs were deposited on the surface of pre-prepared semiconductor particles upon UV-light irradiation [28,29]. Gu et al. prepared ZnO/Ag heterostructures by a two-step chemical method, in which the ZnO were deposited on the surface of pre-synthesized Ag nanowires [30]. The co-precipitation, solvothermal, electrospun and templated methods are also effective in constructing the composites [31–33]. These works demonstrated that the combination of Ag with ZnO is effective for

* Corresponding author. Fax: +86 451 86608458.
E-mail address: fuhg@vip.sina.com (H. Fu).

0022-4596/$ - see front matter © 2010 Elsevier Inc. All rights reserved.
doi:10.1016/j.jssc.2010.09.020

designing the photocatalysts with improved performance. Nevertheless, multi-step procedure needed in some synthesis make the preparation complex. On the other hand, the challenge in one-pot synthesis is how to control the growth of Ag NPs on the surface of ZnO. As known, the photocatalysis is a surface reaction process [1,15]. It therefore is rational to deposit metal NPs on the surface of ZnO for effectively improving the surface properties of ZnO photocatalysts. Thus, an effective route to forming ZnO particles with Ag nanoparticles on the surface would be an important development to extend the use of zinc oxide as a photocatalyst.

Taking advantage of the multifunctional characteristics of the reagents can simplify the synthesis of nanostructured materials [34–36]. The use of the ethylene glycol (EG) as reducing reagent is well demonstrated in the synthesis of the metal NPs [37]. On the other hand, the EG can also act as a media in the preparation of the metal oxides via forced hydrolysis of metal salts [38,39]. In the present study, we proposed a straightforward "one-pot" strategy for preparing Ag/ZnO composites by taking multifunctional characteristics of the EG. Experimental results indicated that the Ag/ZnO microspheres (Ag NPs modified ZnO microspheres) could be obtained through a "one-pot" reaction, in which the $Zn(Ac)_2 \cdot 2H_2O$ and $AgNO_3$ were added into the EG in succession. X-ray powder diffraction (XRD), UV–vis, scanning electron microscopy (SEM) and transmission electron microscopy (TEM) analyses indicated the successful growth of Ag NPs on the surface of the ZnO spheres. Furthermore, the photocatalytic test indicated that the Ag/ZnO composites exhibited better photocatalytic performance than the commercial TiO_2 catalyst (P25) for photodegradation of Rhodamine B (RhB) dye. After reused for 5 times, there are no obvious decrease in the photocatalytic activity of Ag/ZnO microspheres. The enhancement reasons of photocatalytic performance also were investigated primary by combination of the photoluminescence with surface photovoltage techniques.

2. Experimental section

2.1. Chemicals

Zinc acetate dihydrate ($Zn(CH_3COOH)_2 \cdot 2H_2O$, $Zn(Ac)_2 \cdot 2H_2O$), ethylene glycol (EG) and silver nitrate ($AgNO_3$) were purchased from Tianjin Kermel Chemical Reagent Co., Ltd. All reagents were used as received without further purification.

2.2. The preparation of Ag/ZnO microspheres

The Ag/ZnO microspheres were fabricated via a "one-pot" process in EG medium. In a typical synthesis, 10 mmol $Zn(Ac)_2 \cdot 2H_2O$ were added into 50 EG in a 100 mL round-bottomed flask. The solution was heated to 160 °C at the rate of 5 °C/min. After reaction was performed at 160 °C for 8 h, 0.25 mmol $AgNO_3$ was added into the suspension, and the reaction was further preceded for 0.5 h. After naturally cooling to room temperature, the products were collected by centrifugation and washed with deionized water for three times. The sample was denoted as X%Ag/ZnO (2.5%Ag/ZnO for this sample), where the X is the molar ratio of Ag to ZnO calculated on the basic of the initial amount of $AgNO_3$ and $Zn(Ac)_2 \cdot 2H_2O$. The 0.0625%Ag/ZnO, 1.25%Ag/ZnO and 5%Ag/ZnO composites also were prepared by tuning the initial ratio of $AgNO_3$ to $Zn(Ac)_2 \cdot 2H_2O$.

2.3. Characterizations

Scanning electron microscopy (SEM, Hitachi S-4800) operated with an acceleration voltage of 5 kV, and transmission electron microscopy (TEM, JEOL-2100) with an acceleration voltage of 200 kV was used to characterize the size and morphology of the products. X-ray powder diffraction (XRD) were performed with a Rigaku (Japan) D/MAX-*r*A X-ray diffractionmeter equipped with graphite monochromatized Cu*K*α radiation ($\gamma = 1.541874$ Å). UV–vis diffuse-reflectance spectra (DRS) were recorded with a UV–vis 2550 spectrometer. Photoluminescence (PL) spectra were recorded with a PE LS-55 spectrofluorophotometer. Surface photovoltage spectra (SPS) measurement of the samples was carried out with a home-built apparatus [40]. The raw SPS data were normalized using the illuminometer (Zolix UOM-1S, made in China).

2.4. The photocatalytic tests

The photocatalytic performance was evaluated by using RhB as a representative dye pollutant. In detail, 0.04 g catalyst (X%Ag/ZnO) and 40 mL of 1.0×10^{-5} mol/L RhB aqueous solution was mixed in a 100 mL cylinder reaction. After stirring under dark for 30 min to reach the adsorption equilibrium, the mixture was irradiated with 15-W UV light-tube (365 nm) for a given time under stirring continuously. After the reaction is completed, the solids were separated by centrifugation. A UV-2550 spectrometer was used to measure the concentration of RhB solution before and after photocatalytic reaction, by mean of the optical characteristic adsorption of RhB solution at about 554 nm. As reference, the photocatalytic activity of P25 was also tested under otherwise same conditions. The pH value of catalyst solution is about 6.

3. Results and discussion

3.1. Structure characterization

Ag/ZnO microspheres were prepared by a one-pot process in which the $Zn(Ac)_2 \cdot 2H_2O$ and $AgNO_3$ were sequentially adding into the EG. The success of the one-pot strategy should be mainly contributed into the two important role of the EG: it could act as a medium for the formation of ZnO microspheres, and reduce the Ag ions to form Ag NPs at the same time (Scheme 1). The possible reaction formulas were given as follows (formula 1 for ZnO, formula 2 and 3 for Ag):

$$Zn(CH_3COO)_2 + H_2O \rightarrow ZnO + 2CH_3COOH \quad (1)$$

$$HOCH_2CH_2OH \leftrightarrows CH_3CHO + H_2O \quad (2)$$

$$CH_3CHO + 2AgNO_3 + H_2O \rightarrow 2Ag + 2HNO_3 + CH_3COOH \quad (3)$$

The sequential addition of $Zn(Ac)_2 \cdot 2H_2O$ and $AgNO_3$ is important for the growth of Ag NPs on ZnO surface. The formation of ZnO and Ag components could be obviously seen from the change of system color. The white solids (ZnO) emerged after adding $Zn(Ac)_2 \cdot 2H_2O$ into EG solvent and reaction for several hours, while the solution changed into the yellow after adding $AgNO_3$ into the system, indicating the formation of Ag NPs. The typical sample, 2.5%Ag/ZnO, was studied by technique of XRD, UV–vis DRS spectroscopy, SEM and TEM. Fig. 1a shows XRD

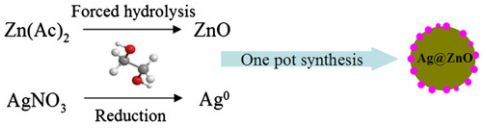

Scheme 1. Schematic procedure for preparation of the Ag/ZnO microspheres.

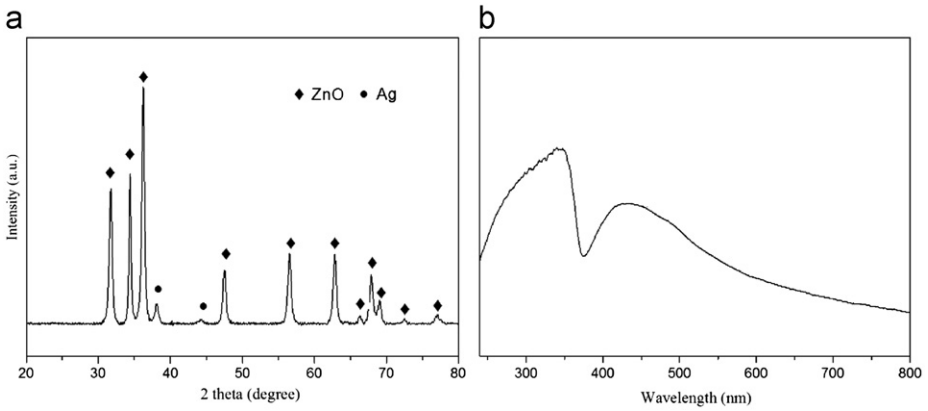

Fig. 1. (a) XRD pattern and (b) UV–vis DRS spectrum of 2.5%Ag/ZnO composites.

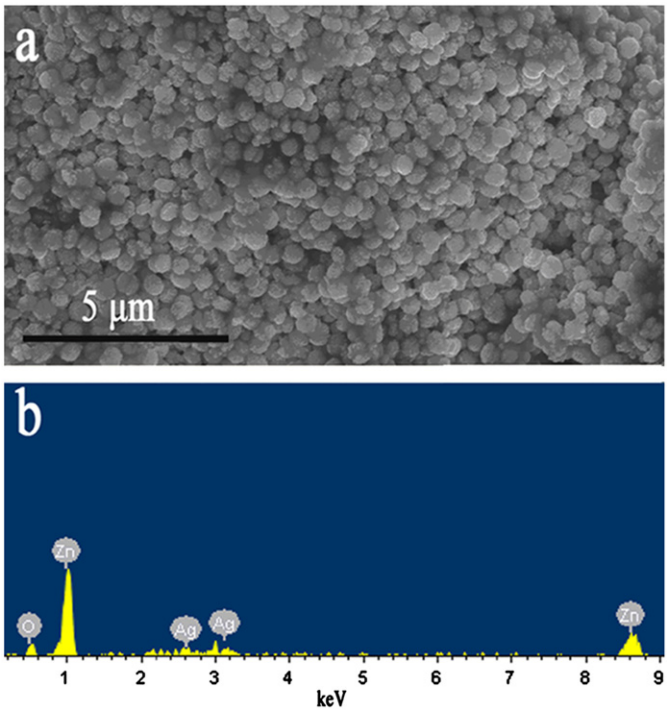

Fig. 2. (a) SEM and (b) EDS of 2.5%Ag/ZnO microspheres.

pattern of the sample. The peaks located at $2\theta=31.7^\circ$, 34.4°, 36.2°, 47.5°, 56.6°, 62.8° and 67.8° are indexed to the (100), (002), (101), (102), (110), (103) and (112) diffractions of ZnO crystals with a hexagonal wurtzite structure, respectively (JCPDS card no. 36-1451). The peaks located at $2\theta=38.2^\circ$ and 44.4° are characteristic diffractions of face-centered-cubic (fcc) structured metal Ag (JCPDS card no. 04-0783). In UV–vis DRS spectra shown in Fig. 1b, two absorption bands are observed. The former can be assigned to absorption of ZnO crystals with corresponding absorption edge at around 375 nm. The peak at about 420 nm is ascribed to surface plasmon absorption of the silver clusters [33]. The spectra of Ag/ZnO microspheres demonstrate also the presence of Ag and ZnO component in as-synthesized sample.

The morphology of 2.5%Ag/ZnO composites was studied with SEM and TEM techniques. Fig. 2a shows an SEM image of 2.5%Ag/ZnO composites. We can see that the sample mainly consists of sphere-like particles with diameters about 500 nm. The peaks corresponding to Ag, Zn and O were observed in the EDX (Energy dispersive X-ray spectroscopy) patterns (Fig. 2b), revealing the formation of Ag/ZnO composites. TEM image (Fig. 3a) shows that the sphere-like particles with diameter about 500 nm are mainly products. Bright field STEM (BF-STEM) images (Fig. 3b) indicate the presence of many small Ag particles (blacker dots with size about 10 nm) on the surface of the microspheres. Corresponding element mapping images (Fig. 3c–e) indicate the presence of Zn, O and Ag elements in single microspheres, demonstrating further the formation of Ag/ZnO microspheres. Also, we rarely observed free Ag NPs based on analyzing a large number of TEM images, showing the successful combination of Ag NPs with ZnO particles. In addition, the amount of Ag in the composites could be easily tuned by changing the initial molar ratio of $AgNO_3$ and $Zn(Ac)_2$ $2H_2O$. Fig. 4 shows XRD patterns of Ag/ZnO microspheres with different ratios of Ag to ZnO. XRD pattern of pure ZnO also is given (Fig. 4a). The characteristic peaks of ZnO can be obviously seen from all patterns. However, the diffraction peaks of metal Ag are not obvious for 0.625%Ag/ZnO due to the low Ag amount in the composites (Fig. 4b). For 1.25%Ag/ZnO, 2.5%Ag/ZnO and 5%Ag/ZnO composites, the peaks located at $2\theta=38.2^\circ$ and 44.4° could be obviously seen as shown in Fig. 4c, a, d, respectively. The size of Ag particle calculated by the Debye–Scherrer formula is about 10.2, 11.5 and 12.8 nm for 1.25%Ag/ZnO, 2.5%Ag/ZnO and 5%Ag/ZnO sample, respectively. At the same time, the relative peak intensity of Ag phase gradually increases with the increase of Ag amount in the composites.

3.2. Study on the photocatalytic activity

The combination of metal NPs with semiconductor oxides is particularly interesting for photocatalytic applications. The photocatalytic activity of Ag/ZnO composites was evaluated by taking RhB as the target dye pollutant. Fig. 5 shows the photodegradation curves of RhB in the presence of different catalysts (Ag/ZnO, ZnO and P25). Under dark conditions, the concentration of RhB has no obvious change for long time in the presence of the catalysts. Similar result was obtained when reaction was performed under UV-light irradiation but without using any catalysts. The results indicate that both the light and ZnO are necessary for effective photodegradation of RhB dye. The photocatalytic process was monitored by chosen the characteristic absorption peaks of RhB at about $\lambda=554$ nm. With the increase of the photo-irradiation time, the absorption peaks of RhB decrease gradually and finally disappear in the presence of Ag/ZnO photocatalysts. The results indicate that Ag/ZnO composites can work as effective photocatalysts. The content of Ag in the composites has obvious influence on the photocatalytic activity. As shown in Fig. 5, the photodegradation efficiency of RhB is about 55%, 86%, 90%, 100% and 82% for ZnO, 0.625%Ag/ZnO, 1.25%Ag/ZnO, 2.5%Ag/ZnO and

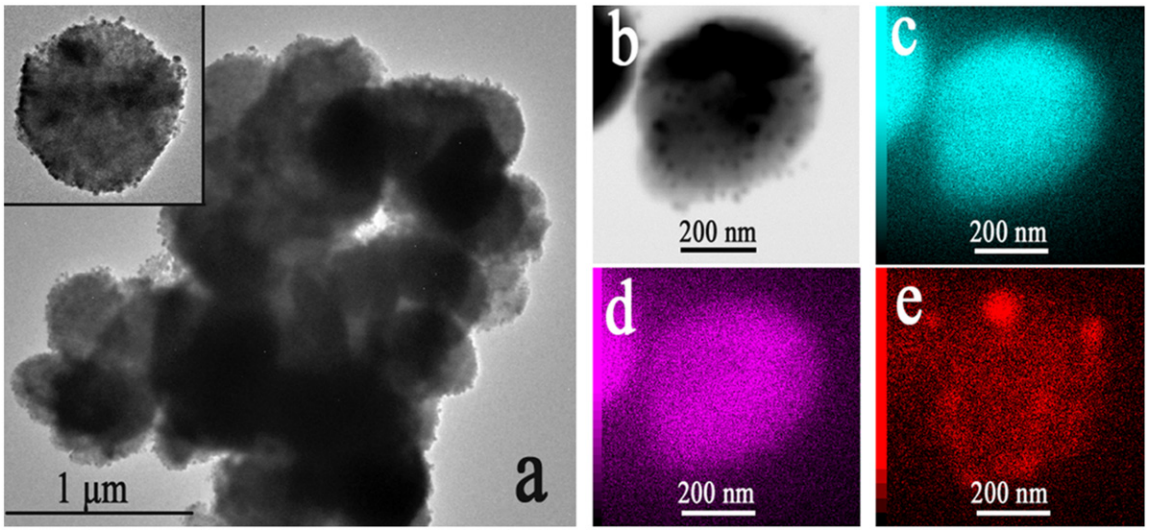

Fig. 3. (a) A low-magnified TEM image of Ag/ZnO composites (inset is TEM image of single Ag/ZnO particle), (b) BF-STEM image of the 2.5%Ag/ZnO microspheres and the corresponding EDS maps, (c) Zn, (d) O and (e) Ag.

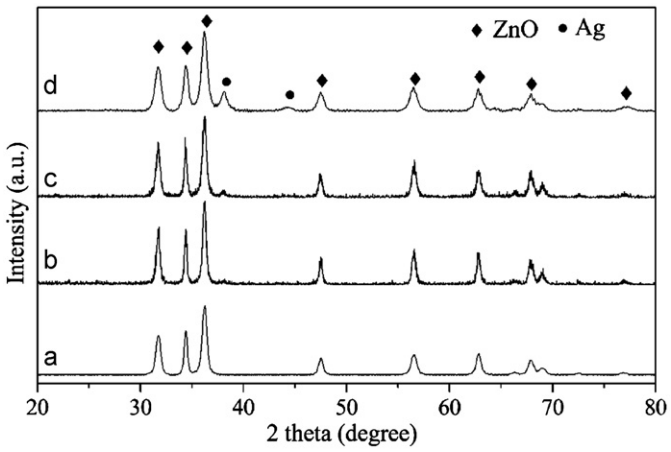

Fig. 4. XRD patterns of (a) ZnO, (b) 0.625%Ag/ZnO, (c) 1.25%Ag/ZnO and (d) 5%Ag/ZnO.

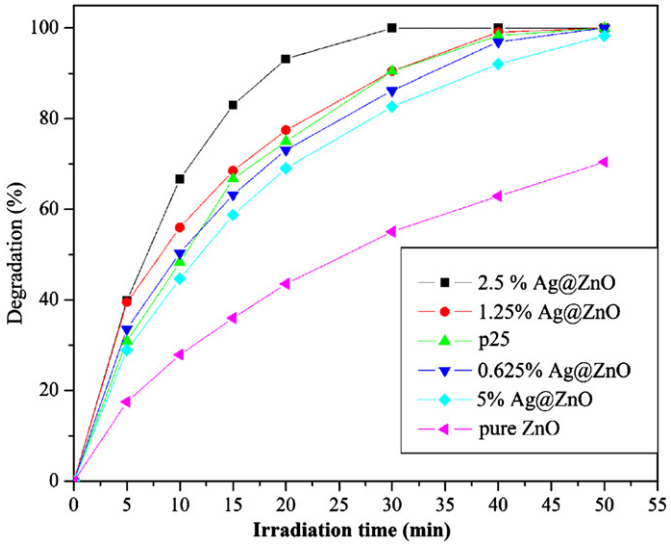

Fig. 5. Photodegradation curve of Rhodamine B under UV-light in the presence of different catalysts.

5%Ag/ZnO, respectively, when the reaction was performed under UV-light for 30 min. It can be seen that ZnO exhibits lowest efficiency among all catalysts. This indicates the importance of Ag modification for improving photocatalytic performance of ZnO. On the other hand, the photodegradation efficiency of RhB increase with the order of ZnO < 5%Ag/ZnO < 0.625%Ag/ZnO < 1.25%Ag/ZnO < 2.5%Ag/ZnO. We can see that the activity of Ag/ZnO composites firstly increased and then decreased with the increase of Ag amount in the composites. The deposition of Ag clusters with appropriate amount on ZnO surface can effectively capture and transfer the photogenerated electrons, and thus suppress the recombination of the electron–hole pairs. However, as more Ag was used, the aggregation and/or size increase of the Ag particles will happen, which is disadvantageous to inhibit the recombination of the electron–hole pairs. To evaluate the photocatalytic activity of Ag/ZnO microspheres further, control experiments in the presence of P25, a recognized material with superior photocatalytic performance, is performed. As shown, the degradation percentage of RhB by P25 catalyst is about 90% after irradiation for 30 min, which is lower than that by 2.5%Ag/ZnO catalyst. Total degradation of RhB by 2.5%Ag/ZnO is realized for about 30 min, while it was reached for 50 min by P25 catalyst. The results indicate that Ag/ZnO composites are superior to P25 for photodegradation of RhB dye.

The recycled performance of the catalyst is also studied on the basic of its importance for practical application. As known, one of the major drawbacks of ZnO photocatalysts is their photocorrosion under UV irradiation [41], which result in significant decrease of the photocatalytic activity in reused process. The modification of ZnO with other materials, such as polyaniline [42] and C_{60} [43], could enhance the photostability that was reflected usually by the good recycled performance of the photocatalysts. Although many works concentrated into the metal/semiconductor composites, the recycled performance of the photocatalysts has been seldom investigated. In the present work, the photocatalytic activity of Ag/ZnO microspheres in recycled process was also studied by taking 2.5%Ag/ZnO catalyst as a typical sample. In reused process, the catalyst was recollected by centrifugation and then re-dispersed in the same RhB aqueous solution for next cycle. Other experimental parameters are same as the first testing. The irradiation time for each test was 30 min. As shown in Fig. 6, the photodegradation efficiency of RhB is about 100% after five reuses of Ag/ZnO photocatalyst. There is no obvious change in photocatalytic activity for 2.5%Ag/ZnO

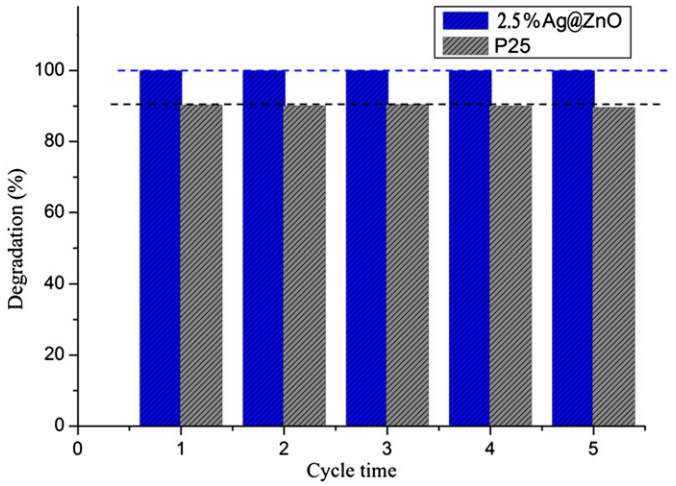

Fig. 6. Recycled performances of 2.5%Ag/ZnO composites and P25 TiO_2 for the photodegradation of RhB dye.

composites. However, for pure ZnO, the photodegradation efficiency of dye in second cycle is decreased about 5% compared to that in first use. The results indicated that the reused activity of ZnO could be improved after Ag modification. As reference, the reused performance of P25 was also investigated. As shown, the degradation efficiency of RhB is about 89% in fifth cycles for P25 catalyst. Slight decrease in the photocatalytic efficiency should be relative with the adsorption of organic molecular on the P25 surface. Also, it is difficult to totally separate the P25 from the system even with assistant of the high-speed centrifugation as its excellent dispersion in water. This leads to the losing of P25, and consequently, the decrease of its photocatalytic activity in recycled process. In contrast, the Ag/ZnO composites could easily settle from reaction system within 10 min, even with no need of centrifugation, because the larger particle size of the composites. This is beneficial for separation and reuse of catalysts. It is obvious that Ag/ZnO composites are suitable photocatalysts due to its high activity, good recycled performance companied by its easy separation from reaction system.

3.3. SPS and PL measurements

The photocatalysis is one of the special photochemical processes. The phtocatalytic activity of materials is closely related with the recombination rate of the photoinduced electrons and holes. Thus, the techniques that can provide the information about the recombination rate of the photoinduced electrons and holes are useful to evaluate the photocatalytic performance of the materials. PL and surface photovoltage (SPV) are two kinds of photophysical phenomena. SPV method relies on analyzing illumination-induced changes in the surface voltage, and it is a well-established contactless and nondestructive technique for semiconductor characterization [40,44]. The photovoltage generated mainly from the creation of electron–hole pairs, followed by separation of them under a built-in electric field. Thus, the SPV spectra (SPS) can reflect photogenerated charge separation and transfer behavior. On the other hand, PL technique has been widely used to investigate the structure and surface property of the metal oxides [45]. For nanostructured materials, the PL spectra are related to the transfer behavior of the photoinduced electrons and holes so that it can reflect the separation and recombination of the photogenerated carriers. Therefore, the SPS and PL could be used to primarily estimate the recombination rate of the photoinduced electron–hole pairs. In another word, they are useful to evaluate the photocatalytic performance of the semiconductor materials [14,36].

The SPS responses of pure ZnO and Ag/ZnO composites are shown in Fig. 7. One obvious SPS response peak can be seen for all samples at about 370 nm. The strong SPS response can be indexed to the electron transitions from the valence band to conduction band (O_{2p}–Zn_{3d}), referred to the energy band structure of ZnO. It can be seen that the SPS peak of ZnO become weak after Ag modification. This indicates that Ag NPs on ZnO surface can act as traps to capture the photoinduced electron, and thus inhibit the recombination of electron–hole pairs. Therefore, the SPS response intensity decreases on the basis of the SPS principle. In addition, it can be found that the amount of Ag has great effect on SPS intensity. In detail, the SPS response becomes gradually weak as the Ag amount increases up to 2.5%. However, the SPS response become strong as the Ag amount is too much (here 5%). This should be contributed to the aggregation and/or size increase of Ag NPs on ZnO surface, resulting in the decrease in ability to trap the photoinduced electrons. Fig. 8 shows PL spectra of pure ZnO and Ag/ZnO composites excited with light of 300 nm wavelengths.

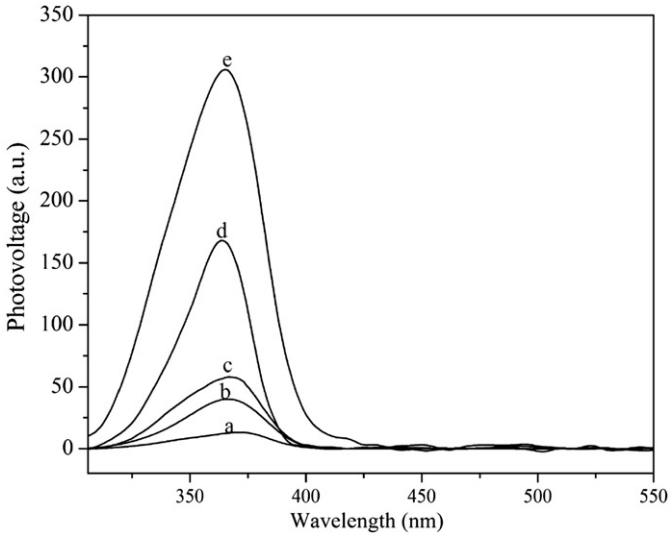

Fig. 7. SPS spectra of (a) 2.5%Ag/ZnO, (b) 1.25%Ag/ZnO, (c) 0.625%Ag/ZnO, (d) 5%Ag/ZnO and (e) ZnO.

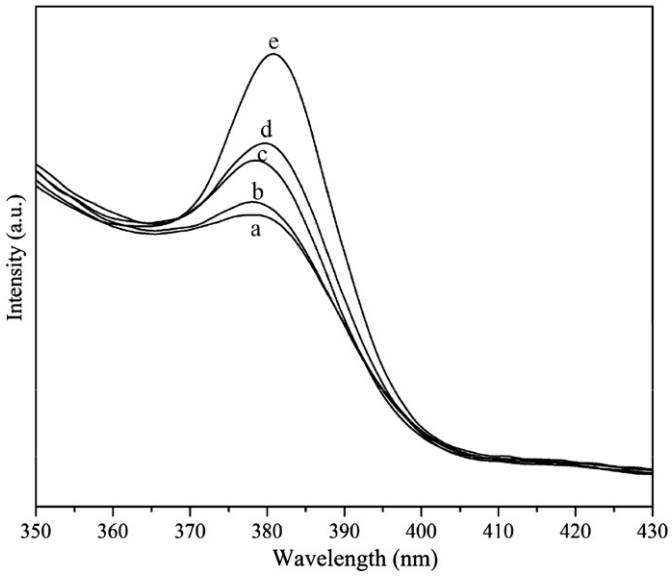

Fig. 8. PL spectra of (a) 2.5%Ag/ZnO, (b) 1.25%Ag/ZnO, (c) 0.625%Ag/ZnO, (d) 5%Ag/ZnO and (e) ZnO.

The energy of used excitation light is enough to promote electronic transitions from the VB to the CB of ZnO according to the above DRS spectrum (Fig. 1b). It can be seen that all the samples exhibit an obvious PL signal at about 378 nm, corresponding to the ultraviolet emission of ZnO particles. From PL spectra, we can found that (1) the PL intensity decrease after the deposition of Ag on the ZnO surface, indicating that Ag NPs on ZnO surface can inhibit the recombination of electron–hole pairs, and (2) PL intensity increase as the more Ag was used (for example 5%), contributing to the aggregation (or size increase) of Ag NPs in the composites. This is disadvantageous to trap the photoelectrons. Based on the above analyses, therefore, it is suggested that Ag modification can make the intensity of PL and SPS decrease. The weaker is PL and SPS response, the better is the separation efficiency of photoinduced electron–hole pairs, and the higher will be the photocatalytic performance of Ag/ZnO composites.

4. Conclusions

The Ag/ZnO composites were successfully prepared through a one pot process in EG system. The composites could act as superior photocatalysts for degradation of organic dye in water with high activity and good stability. PL and SPS studies indicated that the deposition of Ag NPs on ZnO surface could effectively inhibit the recombination of photoinduced electron–hole pairs. With appropriate ratio of Ag and ZnO, the Ag/ZnO composites exhibited the superior photocatalytic ability to P25. The present methods are promising for constructing Ag–ZnO composites in a simple "one-pot" route. This synthetic approach may find application in preparation of other kinds of metal/semiconductor composites, given the versatility of ethylene glycol in the preparation of metal NPs and semiconductor oxides.

Acknowledgments

We gratefully acknowledge the support of the Key Program Projects of the National Natural Science Foundation of China (no. 21031001), the National Natural Science Foundation of China (nos. 20971040 and 21001042), the Cultivation Fund of the Key Scientific and Technical Innovation Project, Ministry of Education of China (no. 708029), the China Postdoctoral Science Foundation (no. 20080440919), the Heilongjiang Postdoctoral Grant (no. LBH-Z08040), and the supporting plan for Excellent Youth of Common Universities of Heilongjiang province of China (no. 1154G24), Doctoral Research Foundation of Heilongjiang University and Youth Science Foundation of Heilongjiang University (QL200711).

References

[1] M.R. Hoffmann, S.T. Martin, W.Y. Choi, D.W. Bahnemann, Chem. Rev. 95 (1995) 69–96.
[2] D. Ravelli, D. Dondi, M. Fagnoni, A. Albini, Chem. Soc. Rev. 38 (2009) 1999–2011.
[3] K. Kabra, R. Chaudhary, R.L. Sawhney, Ind. Eng. Chem. Res. 43 (2004) 7683–7696.
[4] F. Han, V.S.R. Kambala, M. Srinivasan, D. Rajarathnam, R. Naidu, Appl. Catal. A: Gen. 359 (2009) 25–40.
[5] U.I. Gaya, A.H. Abdullah, J. Photochem. Photobiol. C: Photochem. Rev. 9 (2008) 1–12.
[6] J.G. Yu, X.X. Yu, Environ. Sci. Technol. 42 (2008) 4902–4907.
[7] M.D. Hernández-Alonso, F. Fresno, S. Suárez, J.M. Coronado, Energy Environ. Sci. 2 (2009) 1231–1257.
[8] L.P. Xu, Y.L. Hu, C. Pelligra, C.H. Chen, L. Jin, H. Huang, S. Sithambaram, M. Aindow, R. Joesten, S.L. Suib, Chem. Mater. 21 (2009) 2875–2885.
[9] B.X. Li, Y.F. Wang, J. Phys. Chem. C 114 (2010) 890–896.
[10] L.Q. Jing, Y.C. Qu, B.Q. Wang, S.D. Li, B.L. Jiang, L.B. Yang, W. Fu, H.G. Fu, J.Z. Sun, Sol. Energy Mater. Sol. Cells 90 (2006) 1773–1787.
[11] S. Cho, S. Kim, J.W. Jang, S.H. Jung, E. Oh, B.R. Lee, K.H. Lee, J. Phys. Chem. C 113 (2009) 10452–10458.
[12] G. Wang, D. Chen, H. Zhang, J.Z. Zhang, J.H. Li, J. Phys. Chem. C 112 (2008) 8850–8855.
[13] G. Ramakrishna, H.N. Ghosh, Langmuir 19 (2003) 3006–3012.
[14] Y.H. Zheng, C.Q. Chen, Y.Y. Zhan, X.Y. Lin, Q. Zheng, K.M. Wei, J.F. Zhu, Y.J. Zhu, Inorg. Chem. 46 (2007) 6675–6682.
[15] E.S. Jang, J.H. Won, S.J. Hwang, J.H. Choy, Adv. Mater. 18 (2006) 3309–3312.
[16] A. Mclaren, T. Valdes-Solis, G.Q. Li, S.C. Tsang, J. Am. Chem. Soc. 131 (2009) 12540–12541.
[17] J. Zheng, Z.Y. Jiang, Q. Kuang, Z.X. Xie, R.B. Huang, L.S. Zheng, J. Solid State Chem. 182 (2009) 115–121.
[18] A.L. Linsebigler, G.Q. Lu, J.T. Yates, Chem. Rev. 95 (1995) 735–758.
[19] F. Caruso, Adv. Mater. 13 (2001) 11–22.
[20] P. Wang, T.F. Xie, H.Y. Li, L. Peng, Y. Zhang, T.S. Wu, S. Pang, Y.F. Zhao, D.J. Wang, Chem. Eur. J. 15 (2009) 4366–4372.
[21] H. Zhang, X.J. Lv, Y.M. Li, Y. Wang, J.H. Li, ACS Nano 4 (2010) 380–386.
[22] Y.N. Xia, Y.J. Xiong, B. Lim, S.E. Skrabalak, Angew. Chem. Int. Ed. 48 (2009) 60–103.
[23] V. Subramanian, E. Wolf, P.V. Kamat, J. Phys. Chem. B 105 (2001) 11439–11446.
[24] H. Zhang, G. Wang, D. Chen, X.J. Lv, J.H. Li, Chem. Mater. 20 (2008) 6543–6549.
[25] H. Zeng, P. Liu, W. Cai, S. Yang, X. Xu, J. Phys. Chem. C 112 (2008) 19620–19624.
[26] J. Yuan, E.S.G. Choo, X.S. Tang, Y. Sheng, J. Ding, J.M. Xue, Nanotechnology 21 (2010) 185606, 10pp.
[27] P. Pawinrat, O. Mekasuwandumrong, J. Panpranot, Catal. Commun. 10 (2009) 1380–1385.
[28] C. Pacholski, A. Kornowski, H. Weller, Angew. Chem. Int. Ed. 43 (2004) 4774–4777.
[29] L.Q. Jing, D.J. Wang, B.Q. Wang, S.D. Li, B.F. Xin, H.G. Fu, J.Z. Sun, J. Mol. Catal. A: Chem. 244 (2006) 193–200.
[30] C.D. Gu, C. Cheng, H.Y. Huang, T.L. Wong, N. Wang, T.Y. Zhang, Cryst. Growth Des. 9 (2009) 3278–3285.
[31] Y.H. Zheng, C.Q. Chen, Y.Y. Zhan, X.Y. Lin, Q. Zheng, K.M. Wei, J.F. Zhu, J. Phys. Chem. C 112 (2008) 10773–10777.
[32] D.D. Lin, H. Wu, R. Zhang, W. Pan, Chem. Mater. 21 (2009) 3479–3484.
[33] Y.H. Zheng, L.R. Zheng, Y.Y. Zhan, X.Y. Lin, Q. Zheng, K.M. Wei, Inorg. Chem. 46 (2007) 6980–6986.
[34] X.P. Sun, S.J. Dong, E.K. Wang, Angew. Chem. Int. Ed. 43 (2004) 6360–6363.
[35] C.G. Tian, Z.H. Kang, E.B. Wang, B.D. Mao, S.H. Li, Z.M. Su, L. Xu, Nanotechnology 17 (2006) 5681–5685.
[36] C.G. Tian, B.D. Mao, E.B. Wang, Z.H. Kang, Y.L. Song, C.L. Wang, S.H. Li, J. Phys. Chem. C 111 (2007) 3651–3657.
[37] B. Wiley, Y.G. Sun, Y.N. Xia, Acc. Chem. Res. 40 (2007) 1067–1076.
[38] D. Jezequel, J. Guenot, N. Jouini, F. Fievet, J. Mater. Res. 10 (1995) 77–83.
[39] I.R. Collins, S.E. Taylor, J. Mater. Chem. 2 (1992) 1277–1281.
[40] L.Q. Jing, X.J. Sun, J. Shang, W.M. Cai, Z.L. Xu, Y.G. Du, H.G. Fu, Sol. Energy Mater. Sol. Cells 79 (2003) 133–151.
[41] A.V. Dijken, A.H. Janssen, M.H.P. Smitsmans, D. Vanmaekelbergh, A. Meijerink, Chem. Mater. 10 (1998) 3513–3522.
[42] H. Zhang, R.L. Zong, Y.F. Zhu, J. Phys. Chem. C 113 (2009) 4605–4611.
[43] H.B. Fu, T.G. Xu, S.B. Zhu, Y.F. Zhu, Environ. Sci. Technol. 42 (2008) 8064–8069.
[44] B.F. Xin, L.Q. Jing, Z.Y. Ren, B.Q. Wang, H.G. Fu, J. Phys. Chem. B 109 (2005) 2805–2809.
[45] M. Iwamoto, H. Furukawa, K. Matsukami, T. Takenaka, S. Kagawa, J. Am. Chem. Soc. 105 (1983) 3719–3720.